Optimum Trajectory Planning for Multi-Rotor UAV Relays with Tilt and Antenna Orientation Variations

Daniel Bonilla Licea[1], Giuseppe Silano[1], Mounir Ghogho[2], and Martin Saska[1]

***Abstract*—Multi-rotor Unmanned Aerial Vehicles (UAVs) need to tilt in order to move; this modifies the UAV's antenna orientation. We consider the scenario where a multi-rotor UAV serves as a communication relay between a Base Station (BS) and another UAV. We propose a framework to generate feasible trajectories for the multi-rotor UAV relay while considering its motion dynamics and the motion-induced changes of the antenna orientation. The UAV relay's trajectory is optimized to maximize the end-to-end number of bits transmitted. Numerical simulations in MATLAB and Gazebo show the benefits of accounting for the antenna orientation variations due to the UAV tilt.**

***Index Terms*—relay, multi-rotor system, UAV, communication-aware robotics**

I. Introduction

Communications-aware robotics is gaining momentum as evidenced by the steady increase in publications by the robotics [1]–[4] and the communications [5]–[7] communities dealing with mobile robots and communications issues. One reason behind this growing interest is the emergence of the 5G technology that aims to integrate Unmanned Aerial Vehicles (UAVs) in the cellular communications network [8], [9].

It is in this context that we encounter the problem of robotic relay trajectory planning where mobile robots, acting as communications relays, have their trajectories optimized according to some communications criteria. One popular type of robots used as relays is the multi-rotor UAV which requires to tilt in order to move [10]. Thus, when two multi-rotor UAVs, equipped with a single fixed antenna each, communicate while moving, the resulting Signal-to-Noise Ratio (SNR) will depend not only on their positions but also on their tilt. As the tilt of the receiver UAV changes, the Angle of Arrival (AoA), measured w.r.t. the antenna reference frame, also changes and so does the antenna gain experienced by the received signal. In other words, in the case of multi-rotor UAVs communications, the quality of the channel depends not only on the UAV's position but also on its orientation (called attitude in the robotics literature).

In some cases, multi-rotor UAVs hover while relaying data; the UAV's orientation remains constant, and so there are no changes in the communications channel induced by the UAV's orientation. For instance, in [11], we studied the scenario where a quad-rotor hovers to collect data from ground sensors; although the UAV antenna's radiation pattern was taken into account, the antenna orientation remained constant.

In other applications the multi-rotor UAVs relay communicates on the move. The existing studies however disregard the effect of the UAV tilt on the antenna orientation. In [6], the authors consider a multi UAV communications system, but the UAV dynamics are oversimplified, and the antenna radiation pattern is disregarded. In [12], the authors consider a UAV relay between ground users, but the effect of the antenna radiation pattern is overlooked. In [4], [13], we considered scenarios where the multi-rotor UAV communicates while moving; we considered more realistic dynamic models for the multi-rotor UAVs, but we disregarded the antenna radiation pattern.

Works similar to ours involving multi-rotor UAVs relays are found in [14], [15]. However, these papers do not consider the effect of the antenna radiation pattern and use oversimplified dynamic models for the UAVs. In [16], the authors consider the problem of trajectory planning for a ground robotic relay in an indoor scenario, and do take into consideration the antenna radiation pattern of a mobile end-target.

In this paper, we optimize the trajectory of a multi-rotor UAV relay between a ground Base Station (BS) and another moving multi-rotor UAV. We consider the antennas' orientation changes, due to the UAVs changing tilt, on the communications channel. This is done by simultaneously considering the UAV dynamical model and its antenna radiation pattern. To the authors' best knowledge, this is the first time that, in the context of multi-rotor of UAVs communications, the UAV tilt-induced changes in the antenna orientation is accounted for in the trajectory design.

A. Organization

In Sec. II-A, we describe the quad-rotor's dynamics and the communications system. Sec. III presents and analyses the communications-aware trajectory planning problem to be solved. Simulations results are presented in Sec. IV. Finally, conclusions are drawn in Sec. V.

B. Notation

$c_\bullet$ and $s_\bullet$ are short notations for $\cos(\bullet)$ and $\sin(\bullet)$, ${}^k x$ is the value of function x at discrete time k, ${}^k\mathbf{p}^{(n)}$ is the n entry of vector $\mathbf{p}$ evaluated at time instant k.

II. Preliminaries

A. Quad-rotor dynamics

As mentioned above, in this work, UAVs are taken to be multi-rotors, and especially quad-rotors. These UAVs have

[1]Daniel Bonilla Licea, Giuseppe Silano, and Martin Saska are with the Faculty of Electrical Engineering, Czech Technical University in Prague, Czech Republic (email: {bonildan, giuseppe.silano, martin.saska}@fel.cvut.cz).

[2]Mounir Ghogho is with the International University of Rabat, Morocco (email: mounir.ghogho@uir.ac.ma).

This work was partially funded by the European Union's Horizon 2020 research and innovation programme AERIAL-CORE under grant agreement no. 871479, by CTU grant no. SGS20/174/OHK3/3T/13, and by the Czech Science Foundation (GAČR), within research project no. 20-10280S.

the particularity that they can either stay still in the air by hovering, or move towards any desired destination, as long as their dynamics constraints are not violated. In order to move, the quad-rotor needs to tilt; its direction of movement ($\mathbf{p}$), velocity ($\mathbf{v}$) and acceleration ($\mathbf{a}$) depend on its Euler angles [17]: roll (φ), pitch (ϑ) and yaw (ψ).

We consider a discrete-time dynamic model for the quad-rotor; let $T_s \in \mathbb{R}_{\geq 0}$ and $T \in \mathbb{R}_{\geq 0}$ denote the UAV sampling period and trajectory time, respectively, and let $\mathbf{t} = [0, T_s, \ldots, NT_s]^\top \in \mathbb{R}^{N+1}$, with ${}^k\mathbf{t} = kT_s$, $k \in \mathbb{N}_{\geq 0}$, and $NT_s = T$. We also define the state $\mathbf{x}$ and control $\mathbf{u}$ sequences as ${}^k\mathbf{x} = [{}^k\mathbf{p}^{(1)}, {}^k\mathbf{v}^{(1)}, {}^k\mathbf{p}^{(2)}, {}^k\mathbf{v}^{(2)}, {}^k\mathbf{p}^{(3)}, {}^k\mathbf{v}^{(3)}]^\top$ and ${}^k\mathbf{u} = [{}^k\mathbf{a}^{(1)}, {}^k\mathbf{a}^{(2)}, {}^k\mathbf{a}^{(3)}]^\top$, where ${}^k\mathbf{p}^{(j)}$, ${}^k\mathbf{v}^{(j)}$, and ${}^k\mathbf{a}^{(j)}$, with $j = \{1, 2, 3\}$, represent the vehicle's position, velocity, and acceleration at time instant k along the j-axis of the inertial frame O_W, respectively.

In [18], the authors present motion primitives to design trajectories that satisfy the UAV's dynamic constraints. This method allows to generate feasible quad-rotor motion primitives. This method provide the following splines that we will use to account for the dynamics of the quad-rotor UAV:

$$\begin{bmatrix} {}^{k+1}\mathbf{p}^{(j)} \\ {}^{k+1}\mathbf{v}^{(j)} \\ {}^{k+1}\mathbf{a}^{(j)} \end{bmatrix} = \begin{bmatrix} \frac{\alpha}{120}\,{}^k\mathbf{t}^5 + \frac{\beta}{24}\,{}^k\mathbf{t}^4 + \frac{\gamma}{6}\,{}^k\mathbf{t}^3 + {}^k\mathbf{a}^{(j)}\,{}^k\mathbf{t}^2 + {}^k\mathbf{v}^{(j)}\,{}^k\mathbf{t} + {}^k\mathbf{p}^{(j)} \\ \frac{\alpha}{24}\,{}^k\mathbf{t}^4 + \frac{\beta}{6}\,{}^k\mathbf{t}^3 + \frac{\gamma}{2}\,{}^k\mathbf{t}^2 + {}^k\mathbf{a}^{(j)}\,{}^k\mathbf{t} + {}^k\mathbf{v}^{(j)} \\ \frac{\alpha}{6}\,{}^k\mathbf{t}^3 + \frac{\beta}{2}\,{}^k\mathbf{t}^2 + \gamma\,{}^k\mathbf{t} + {}^k\mathbf{a}^{(j)} \end{bmatrix}, \tag{1}$$

where α, β and γ are design parameters that determine the behaviour at the start and end points [18, Appx. A].

B. Communications System

The communications system consists of two communications links: UAV-2 →UAV-1 and UAV-1 →BS. Both UAVs are equipped with a single antenna; we arbitrarily choose the half-wave dipole[1], but the proposed method apply to other types of antennas. The q-th UAV antenna is located at its center of mass $\mathbf{p}_q$, and is aligned to its z_{B_q} axis, see Fig. 1. The gain experienced by the wave transmitted by the q-th UAV's is [19]:

$$G_q(\vartheta) = \frac{D\cos(\cos(\vartheta)\pi/2)}{\sin(\vartheta)}, \quad q = \{1, 2\}, \tag{2}$$

where D is the half-wave dipole's directivity (≈ 1.64), ϑ is the Angle of Departure (AoD) of the radiated wave measured w.r.t. the antenna's axis z_{B_q}. Note that (2) also describes the gain experienced by the received wave, in which case ϑ becomes the Angle of Arrival (AoA).

To highlight the effect of the coupling between the UAVs' tilt and its antenna orientation, we perform the following simplifications: we assume Line of Sight (LoS) for both communications links, we neglect small-scale fading, and we assume that the BS tracks UAV-1 using beamforming. Then, we model the communications channels by using the free space model and including the effect of the antennas' radiation pattern. Thus, the UAV-2 →UAV-1 channel is modeled as:

$$r_1 = \left(\frac{G_2(\vartheta^D_{2,1})G_1(\vartheta^A_{2,1})}{\|\mathbf{p}_2 - \mathbf{p}_1\|}\right) s_2 + n_1, \tag{3}$$

[1]Half-wave dipole is a common type of antenna.

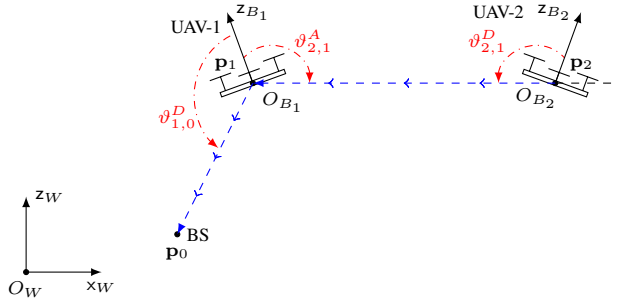

Fig. 1: Multi-rotor UAV-1 as a communications relay between the multi-rotor UAV-2 and the BS.

where r_1 and s_2 are the signals received and transmitted by the UAV-1 and UAV-2, respectively; n_1 is the zero-mean complex Additive White Gaussian Noise (AWGN) with power σ_1^2 generated at the UAV-1's receiver; $\vartheta^D_{2,1}$ and $\vartheta^A_{2,1}$ are the AoD and AoA measured w.r.t. the axes z_{B_2} and z_{B_1}, respectively. Using simple geometry, we have that:

$$\vartheta^D_{2,1} = \arctan\left(\frac{h^{(3)}_{2,1}}{\sqrt{(h^{(1)}_{2,1})^2 + (h^{(2)}_{2,1})^2}}\right) - \frac{\pi}{2}, \tag{4}$$

$$\vartheta^A_{2,1} = \arctan\left(\frac{h^{(3)}_{1,2}}{\sqrt{(h^{(1)}_{1,2})^2 + (h^{(2)}_{1,2})^2}}\right) - \frac{\pi}{2}, \tag{5}$$

where $h^{(r)}_{w,q}$ is the r-element of the vector ${}^W\mathbf{R}_{B_q}(\mathbf{p}_w - \mathbf{p}_q)$ with ${}^W\mathbf{R}_{B_q}$ the rotation matrix from the global (O_W) to the q-th UAV coordinate system [17]. The UAV-1 →BS channel is obtained by performing the following changes on the UAV-2 →UAV-1 channel equations: (i) exchanging the subindexes as follows $2 \to 1$ and $1 \to 0$; (ii) setting $G_0(\vartheta^A_{1,0}) = D_B$ for all $\vartheta^A_{1,0}$ (to model the beamforming implemented by the BS) where D_B is the directivity of the main beam tracking the UAV-1. Finally, we denote $\xi_{2,1}$ and $\xi_{1,0}$ the SNRs of the UAV-2 →UAV-1 and UAV-1 →BS channels, respectively.

III. Problem Statement & Solution

While UAV-2 follows a trajectory $\mathcal{T}_2$ it must transmit data to the BS. To improve the communications and extend UAV-2's range of action, another UAV (i.e., UAV-1) acting as a relay is integrated to the system. We assume that UAV-2 communicates only with UAV-1 which simultaneously relays[2] the data to the BS located at $\mathbf{p}_0$. The end-to-end channel capacity of this system corresponds to the capacity of the channel having the poorest SNR. Now, given $\mathcal{T}_2$, we want to optimize the predetermined UAV-1 trajectory so as to maximize the number of bits transmitted from UAV-2 to

[2]This can be achieved by using Frequency-Division Duplexing (FDD).

the BS via UAV-1. This can be achieved by solving:

$$\begin{aligned}\underset{\mathbf{p}_1,\mathbf{v}_1,\mathbf{a}_1}{\text{maximize}} \quad & \sum_{k=0}^{N} \min\Big(\log_2\Big(1+{}^k\xi_{1,0}\Big), \log_2\Big(1+{}^k\xi_{2,1}\Big)\Big) \\ \text{s.t.} \quad & {}^k\xi_{1,0} = \frac{D_B^2\, G_1^2({}^k\vartheta_{1,0}^D) P}{\|{}^k\mathbf{p}_1 - \mathbf{p}_0\|^2 \sigma_0^2}, \\ & {}^k\xi_{2,1} = \frac{G_1^2({}^k\vartheta_{2,1}^A)\, G_2^2({}^k\vartheta_{2,1}^D) P}{\|{}^k\mathbf{p}_2 - {}^k\mathbf{p}_1\|^2\, \sigma_1^2}, \\ & |{}^k\mathbf{v}^{(j)}| \le \mathbf{v}_{\max}^{(j)}, |{}^k\mathbf{a}^{(j)}| \le \mathbf{a}_{\max}^{(j)}, \\ & \text{eq. (1)}, \forall k = \{0,1,\ldots,N-1\},\end{aligned} \tag{6}$$

where P is the power of the transmitted signal, $\min(\log_2(1+{}^k\xi_{1,0}), \log_2(1+{}^k\xi_{2,1}))$ is the normalized upper bound for the end-to-end data bit rate at discrete time k. The angles $\vartheta_{2,1}^A$ and $\vartheta_{2,1}^D$ are calculated with (4)–(5), while $\vartheta_{1,0}^D$ is also calculated in a similar manner. We want the optimum trajectory (i.e., $\mathbf{p}_1^\star$, $\mathbf{v}_1^\star$, and $\mathbf{a}_1^\star$) obtained after solving the optimization problem (6) to be feasible. We ensure this with the last two lines of constraints in (6) that take into account the dynamics of UAV-1 and its physical constraints, i.e., maximum velocity and acceleration.

Now, we transform the maximization problem (6) into a more standard minimization problem[3]. We achieve this by first replacing the $\max$imize with $\min$imize action and then changing the cost function in (6) to:

$$\bar{J} = \sum_{k=0}^{N} \max\left(\frac{1}{\log_2(1+{}^k\xi_{1,0})}, \frac{1}{\log_2(1+{}^k\xi_{2,1})}\right). \tag{7}$$

After transforming (6) into a minimization problem we note that the $\max$ function in (7) makes the optimization problem NP-hard: to evaluate the $\max$ function in $\bar{J}$ for a single candidate trajectory, the optimization algorithm must compare ${}^k\xi_{1,0}$ with ${}^k\xi_{2,1}$ for all k. To solve this, we approximate the $\max$ function with a smooth function to ensure that the optimization problem is no longer NP-hard. We use the following approximation, see Appendix A:

$$\bar{J} \approx \sum_{k=0}^{N} \left(\frac{1}{\Big(\log_2(1+{}^k\xi_{1,0})\Big)^p} + \frac{1}{\Big(\log_2(1+{}^k\xi_{2,1})\Big)^p}\right)^{1/p}.$$

From (2)–(4) we observe that $G_2^2(\vartheta_{2,1}^D)$ is a highly nonlinear function of $\mathbf{p}_1$; this adds local minima to the optimization problem. We alleviate this by approximating the antenna power gains as follows, see Appendix B:

$$G_2^2(\vartheta_{2,1}^D) \approx D_d^2\, \mathbf{g}(\vartheta_2, \varphi_2)^\top \mathbf{v}_{2,1}, \tag{8}$$

where ϑ_2 and φ_2 are the roll and pitch angles for UAV-2, respectively, $\mathbf{g}(\vartheta_2,\ \varphi_2) = [1,\ -s_{\vartheta_2}^2,\ -c_{\vartheta_2}^2 s_{\varphi_2}^2,\ -c_{\varphi_2}^2 c_{\vartheta_2}^2,\ 2c_{\vartheta_2}s_{\vartheta_2}s_{\varphi_2},\ -2c_{\vartheta_2}c_{\varphi_2}s_{\vartheta_2},\ 2c_{\vartheta_2}^2 c_{\varphi_2}s_{\varphi_2}]^\top$, $(\mathbf{p}_2 - \mathbf{p}_1)/\|\mathbf{p}_2 - \mathbf{p}_1\| = [d_{2,1}^{(1)}, d_{2,1}^{(2)}, d_{2,1}^{(3)}]^\top$, and $\mathbf{v}_{2,1} = [1,\ (d_{2,1}^{(1)})^2,\ (d_{2,1}^{(2)})^2, (d_{2,1}^{(3)})^2, d_{2,1}^{(1)}d_{2,1}^{(2)}, d_{2,1}^{(1)}d_{2,1}^{(3)}, d_{2,1}^{(2)}d_{2,1}^{(3)}]^\top$. In a similar manner:

$$\begin{aligned} G_1^2(\vartheta_{2,1}^A) &\approx D_d^2\, \mathbf{g}(\vartheta_1, \varphi_1)^\top \mathbf{v}_{2,1}, \\ G_1^2(\vartheta_{1,0}^D) &\approx D_d^2\, \mathbf{g}(\vartheta_1, \varphi_1)^\top \mathbf{v}_{1,0}. \end{aligned} \tag{9}$$

Note that the antenna gains (9) depend not only on the position of the UAV-1 (i.e., $\mathbf{p}_1$) but also on its roll (φ_1) and pitch (ϑ_1) angles. Now, we are optimizing the UAV-1 trajectory w.r.t. its position ($\mathbf{p}_1$), velocity ($\mathbf{v}_1$) and acceleration ($\mathbf{a}_1$); these variables implicitly determine the roll and pitch angles throughout the full UAV-1 trajectory [17], [18]. Nevertheless, considering such nonlinear relation would significantly complicate the optimization problem and thus for simplicity, during the optimization, we will evaluate (9) at $\vartheta_1 = \varphi_1 = 0$ which corresponds to the hovering position.

Thus, after all the elements discussed in this section we reformulate the optimization problem (6) as:

$$\begin{aligned}\underset{\mathbf{p}_1,\mathbf{v}_1,\mathbf{a}_1}{\text{minimize}} \quad & \sum_{k=0}^{N} \left(\frac{1}{\log_2^p\Big(1+{}^k\xi_{1,0}\Big)}, \frac{1}{\log_2^p\Big(1+{}^k\xi_{2,1}\Big)}\right)^{1/p} \\ \text{s.t.} \quad & {}^k\xi_{1,0} = \frac{D_B^2\, D^2 \mathbf{g}(\vartheta_1,\varphi_1)^\top \mathbf{v}_{1,0} P}{\|{}^k\mathbf{p}_1 - \mathbf{p}_0\|^2 \sigma_0^2}, \\ & {}^k\xi_{2,1} = \frac{D^4 \mathbf{g}(\vartheta_1,\varphi_1)^\top \mathbf{v}_{2,1} \mathbf{g}(\vartheta_2,\varphi_2)^\top \mathbf{v}_{2,1} P}{\|{}^k\mathbf{p}_2 - {}^k\mathbf{p}_1\|^2\, \sigma_1^2}, \\ & |\mathbf{v}_k^{(j)}| \le \mathbf{v}_{\max}^{(j)}, |\mathbf{a}_k^{(j)}| \le \mathbf{a}_{\max}^{(j)}, \\ & \text{eq. (1)}, \forall k = \{0,1,\ldots,N-1\}, \\ & \text{with } \vartheta_1, \varphi_1 = 0.\end{aligned} \tag{10}$$

IV. Simulations

In this section, we test the trajectory of UAV-1 optimized using the proposed method. The trajectory of UAV-2, $\mathcal{T}_2$, is taken from [20]; it was designed for a power tower inspection task, and was experimentally validated. The position of the BS is $[1.00, 3.00, 1.50]^\top$ and the initial positions for UAV-1 and UAV-2 are $[0.00, 3.00, 1.50]^\top$ and $[4.00, 3.00, 1.50]^\top$, respectively.

The optimization problem (10) is solved using the CASADI library[4] and NLP[5] as solver. The maximum number of iterations is set to 2000, with acceptable tolerance of 1.0×10^{-4}. Simulations were carried out using the 2019b release of MATLAB on a laptop with an i7-8565U processor (1.80 GHz) and 32GB of RAM running on Ubuntu 18.04. Videos with the experiments and numerical simulations in MATLAB and Gazebo are available at http://mrs.felk.cvut.cz/optimum-trajectory-relay.

To show the advantages of considering the antenna orientation changes, due to the UAV tilt in the trajectory optimization we compare two different trajectories: the first trajectory is obtained after solving (10), see Fig. 2; the second trajectory is obtained after solving (10) but disregarding the antenna

[3]After many simulations and numerical analysis we observed that, in this particular case, the maximization problem was difficult to solve and produced erratic trajectories; the minimization formulation produces coherent trajectories. More analysis is required to understand this issue.

[4]https://web.casadi.org

[5]http://cvxr.com

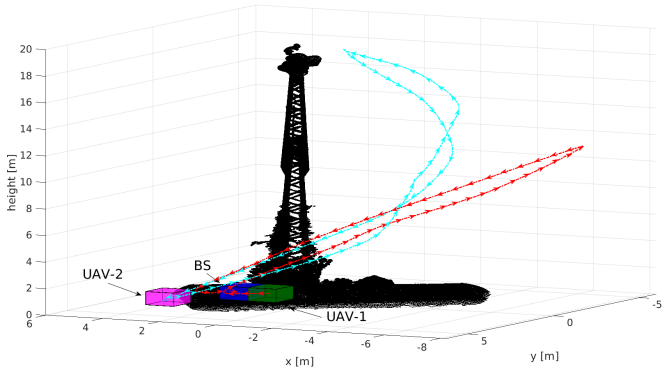

Fig. 2: First UAV-1 trajectory (red) and UAV-2 trajectory (cyan). The BS, UAV-1 and UAV-2 starting points are reported in blue, green and magenta boxes, respectively.

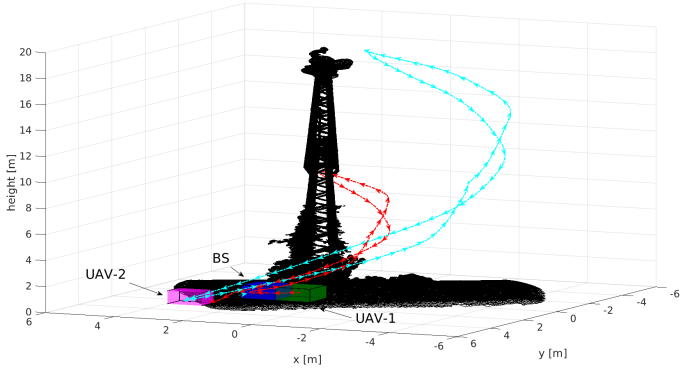

Fig. 3: Second UAV-1 trajectory (red) and UAV-2 trajectory (cyan).

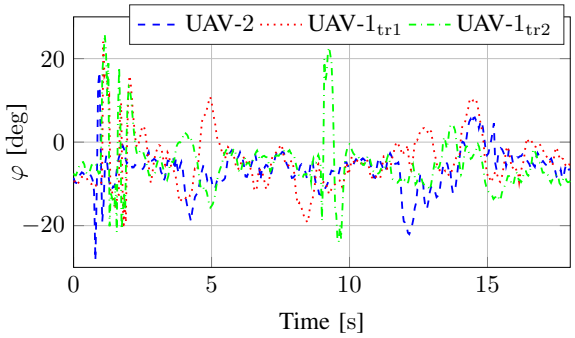

Fig. 4: Roll angle (φ) for the UAV-2 and both UAV-1 trajectories (i.e., UAV-1_{tr1} and UAV-2_{tr2}).

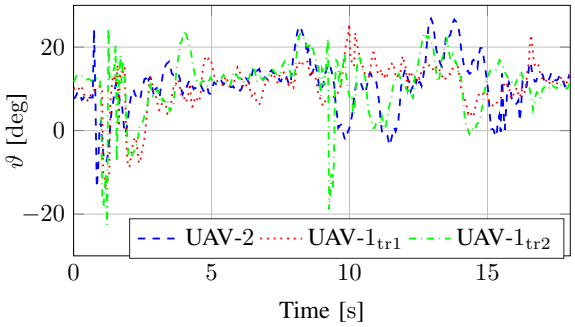

Fig. 5: Pitch angle (ϑ) for the UAV-2 and both UAV-1 trajectories.

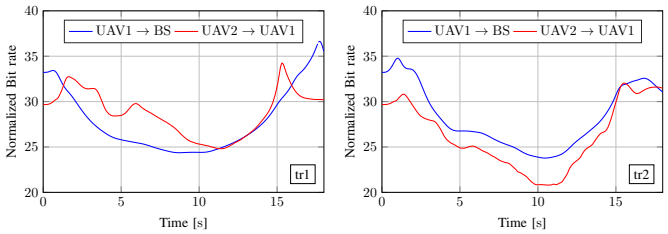

Fig. 6: Instantaneous bit rates of both links for both trajectories: first UAV-1 trajectory (left), second UAV-1 trajectory (right).

radiation patterns[6], see Fig. 3. The time taken by the solver for the first and second trajectories are 154 s and 63 s, respectively. Both trajectories are optimized using the same UAV-2 trajectory $\mathcal{T}_2$ and the following parameter values: $p = 10$, ${}^{D^4P}/_{\sigma_1^2} = 10^9$, ${}^{D_B^2D^2P}/_{\sigma_0^2} = 10^9$, $\mathbf{v}_{\max}^{(j)} = 2\,\mathrm{m\,s^{-1}}$, $\mathbf{a}_{\max}^{(j)} = 2\,\mathrm{m\,s^{-2}}$, sampling time $T_s = 0.05\,\mathrm{s}$ and trajectory duration $T = 18.0\,\mathrm{s}$, and α, β, and γ from [18, eq. (63)]. After obtaining the trajectories in MATLAB we execute them in Gazebo[7] to verify their feasibility and to measure the corresponding realistic roll and pitch angles for both UAV-1 trajectories and for UAV-2 trajectory $\mathcal{T}_2$, see Figs. 4 and 5. These angles provide the reader with an idea about the UAVs antenna orientation.

From Figs. 2 and 3 we note that the first UAV-1 trajectory seems to get away from the UAV-2 and the BS to align itself with the the UAV-2's antenna; the second UAV-1 trajectory simply mimics $\mathcal{T}_2$ in a scaled manner.

The number of bits that can be transmitted, calculated with the optimization target of (10), using the first UAV-1 trajectory is 6.4% higher than that for the second UAV-1 trajectory. In Fig. 6 we see the instantaneous normalized bit rate of both links for both trajectories: the minimum instantaneous bit rate for the first UAV-1 trajectory is 17.3% higher than that for the second UAV-1 trajectory.

Higher gain antennas have lower half-power bandwidth; as the antenna gain increases the UAV relay performance becomes more sensitive to the antenna orientation changes. Additionally, as the multi-rotor UAV moves faster its tilt (and that of its antenna) increases. Hence, higher gain antennas and/or higher UAV speeds increase the relevance of our proposed technique.

V. Conclusions

We presented a framework to design a multi-rotor trajectory considering a realistic dynamic model of the aircraft and the antenna orientation changes due to the UAV tilt. Initial results show that considering the antenna orientation changes during the trajectory optimization can increase the overall number of bits transmitted and the minimum instantaneous bit rate. The

[6]This is done by exchanging $\mathbf{g}(\vartheta_j, \varphi_j)^\top \mathbf{v}_{k,j}$ with 1.

[7]Gazebo is a robotics simulator that uses complex and realistic models for the UAVs; we exploit the advantages of Software-in-the-loop (SIL) simulations [21] by generating the trajectories in MATLAB and then testing them in Gazebo.

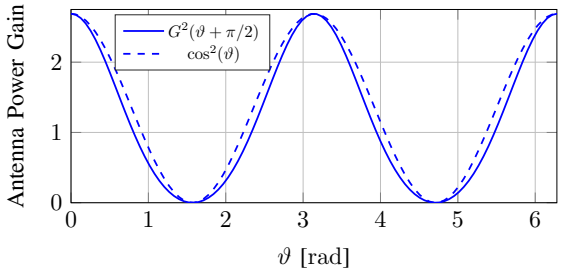

Fig. 7: Half-wave dipole power radiation pattern and its approximation.

actual benefit derived from this consideration depends on the type of antenna and on the UAV trajectories. Future research will determine the characteristics of the trajectories that benefit the most from this approach and also will evaluate the energy efficiency of the resulting trajectories.

Appendix A
Smooth approximation for min function

In this appendix we present a smooth approximation for $\max_j(\varepsilon_j)$. From the definition of the H_∞ norm we have:

$$\|\varepsilon_1, \varepsilon_2, \ldots, \varepsilon_N\|_\infty = \max_{j\in\{1,2,\ldots,N\}} \varepsilon_j. \tag{11}$$

Now, it is well known that p-norm $\rightarrow$ H_∞ norm as $p \rightarrow \infty$ [22]. In other words, $\|\mathbf{u}\|_\infty = \lim_{p\to\infty} \|\mathbf{u}\|_p$, and thus:

$$\|\varepsilon_1, \varepsilon_2, \ldots, \varepsilon_N\|_\infty \approx \|\varepsilon_1, \varepsilon_2, \ldots, \varepsilon_N\|_p = \left(\sum_{j=1}^N \varepsilon_j^p\right)^{\frac{1}{p}}, \tag{12}$$

where the r.h.s. of (12) gets closer to the l.h.s. as $p \in \mathbb{N}^+$ increases. Finally, we have $\max_{j\in\{1,2,\ldots,N\}} \varepsilon_j \approx \left(\sum_{j=1}^N \varepsilon_j^p\right)^{\frac{1}{p}}$.

Appendix B
Antenna Radiation Pattern approximation

Let us consider the UAV-2 $\rightarrow$UAV-1 channel and define the vector $\mathbf{d}_{2,1} \triangleq (\mathbf{p}_2-\mathbf{p}_1)/\|\mathbf{p}_2-\mathbf{p}_1\| = [d_{2,1}^{(1)}, d_{2,1}^{(2)}, d_{2,1}^{(3)}]^\top$, where $\mathbf{d}_{2,1}$ is expressed within the global coordinate system O_W. Then let us define $\underline{\mathbf{d}}_{2,1} \triangleq {}^W\mathbf{R}_{B_q}\mathbf{d}_{2,1}$ with the rotation matrix ${}^W\mathbf{R}_{B_q}$ given as in [17]. Since $\|\mathbf{d}_{2,1}\| = 1$ and the rotation matrix is unitary then $\|\underline{\mathbf{d}}_{2,1}\| = 1$. Let $\hat{\underline{\mathbf{d}}}_{2,1}$ be the projection of $\underline{\mathbf{d}}_{2,1}$ on the plane $\mathcal{H}_q$ spanned by $O_{B_q}\mathsf{x}_{B_q}$ and $O_{B_q}\mathsf{y}_{B_q}$. Now, since we are working on an Euclidean space [23] the inner product between $\hat{\underline{\mathbf{d}}}_{2,1}$ and $\underline{\mathbf{d}}_{2,1}$ is:

$$\langle\hat{\underline{\mathbf{d}}}_{2,1}, \underline{\mathbf{d}}_{2,1}\rangle/\|\hat{\underline{\mathbf{d}}}_{2,1}\| = \cos(\varphi_{2,1}), \tag{13}$$

where $\varphi_{2,1}$ is the angle formed between $\hat{\underline{\mathbf{d}}}_{2,1}$ and $\underline{\mathbf{d}}_{2,1}$ that corresponds to the AoD measured w.r.t. $\mathcal{H}_q$, and $\vartheta_{2,1}$ in (3) is the AoD measured w.r.t. $O_{B_q}\mathsf{z}_{B_q}$. Thus, we have $\cos(\varphi_{2,1}) = \cos(\varphi_{2,1}+\pi/2)$. $\langle\hat{\underline{\mathbf{d}}}_{2,1}, \underline{\mathbf{d}}_{2,1}\rangle = \hat{\underline{\mathbf{d}}}_{2,1}^\top\underline{\mathbf{d}}_{2,1}$ is the inner product of both vectors in the Euclidean space. After some algebra:

$$\langle\hat{\underline{\mathbf{d}}}_{2,1}, \underline{\mathbf{d}}_{2,1}\rangle = \|\hat{\underline{\mathbf{d}}}_{2,1}\|^2 = \mathbf{g}(\vartheta_2, \varphi_2)^\top\mathbf{v}_{2,1}, \tag{14}$$

where $\mathbf{g}(\vartheta_2, \varphi_2) = [1, -s_{\vartheta_2}^2, -c_{\vartheta_2}^2 s_{\varphi_2}^2, -c_{\varphi_2}^2 c_{\vartheta_2}^2, 2c_{\vartheta_2}s_{\vartheta_2}s_{\varphi_2}, -2c_{\vartheta_2}c_{\varphi_2}s_{\vartheta_2}, 2c_{\vartheta_2}^2 c_{\varphi_2}s_{\varphi_2}]^\top$ and $\mathbf{v}_{2,1} = [1, (d_{2,1}^{(1)})^2, (d_{2,1}^{(2)})^2, (d_{2,1}^{(3)})^2, d_{2,1}^{(1)}d_{2,1}^{(2)}, d_{2,1}^{(1)}d_{2,1}^{(3)}, d_{2,1}^{(2)}d_{2,1}^{(3)}]^\top$. It can be observed from Fig. 7 that $G_2^2(\vartheta_{2,1}+\pi/2) \approx D^2\cos^2(\vartheta_{2,1})$; then, considering (13) and (14) we obtain $G_2^2(\vartheta_{2,1}+\pi/2) \approx D^2\mathbf{g}(\vartheta_2, \varphi_2)^\top\mathbf{v}_{2,1}$.

References

[1] A. Gasparri *et al.*, "Bounded Control Law for Global Connectivity Maintenance in Cooperative Multirobot Systems," *IEEE Transactions on Robotics*, vol. 33, no. 3, pp. 700–717, 2017.

[2] V. S. Varadharajan *et al.*, "Swarm Relays: Distributed Self-Healing Ground-and-Air Connectivity Chains," *IEEE Robotics and Automation Letters*, vol. 5, no. 4, pp. 5347–5354, 2020.

[3] D. Bonilla Licea *et al.*, "Mobile Robot Path Planners With Memory for Mobility Diversity Algorithms," *IEEE Transactions on Robotics*, vol. 33, no. 2, pp. 419–431, 2017.

[4] ——, "Communication-Aware Energy Efficient Trajectory Planning With Limited Channel Knowledge," *IEEE Transactions on Robotics*, vol. 36, no. 2, pp. 431–442, 2020.

[5] Y. Zeng *et al.*, "Energy-Efficient UAV Communication With Trajectory Optimization," *IEEE Transactions on Wireless Communications*, vol. 16, no. 6, pp. 3747–3760, 2017.

[6] Q. Wu *et al.*, "Joint Trajectory and Communication Design for Multi-UAV Enabled Wireless Networks," *IEEE Transactions on Wireless Communications*, vol. 17, no. 3, pp. 2109–2121, 2018.

[7] M. T. Dabiri *et al.*, "Optimal Placement of UAV-Assisted Free-Space Optical Communication Systems With DF Relaying," *IEEE Communications Letters*, vol. 24, no. 1, pp. 155–158, 2020.

[8] M. Debashisha *et al.*, "A survey on cellular-connected UAVs: Design challenges, enabling 5G/B5G innovations, and experimental advancements," *Computer Networks*, vol. 182, pp. 1–25, 2020.

[9] Y. Zeng *et al.*, "Accessing From the Sky: A Tutorial on UAV Communications for 5G and Beyond," *Proceedings of the IEEE*, vol. 107, no. 12, pp. 2327–2375, 2019.

[10] R. Mahony *et al.*, "Multirotor Aerial Vehicles: Modeling, Estimation, and Control of Quadrotor," *IEEE Robotics Automation Magazine*, vol. 19, no. 3, pp. 20–32, 2012.

[11] D. Bonilla Licea *et al.*, "Energy-Efficient 3D UAV Trajectory Design for Data Collection in Wireless Sensor Networks," in *IEEE International Conference on Acoustics, Speech and Signal Processing*, 2020, pp. 8329–8333.

[12] S. Ahmed *et al.*, "Energy-Efficient UAV Relaying Communications to Serve Ground Nodes," *IEEE Communications Letters*, vol. 24, no. 4, pp. 849–852, 2020.

[13] D. Bonilla Licea *et al.*, "UAV Trajectory Planning for Delay Tolerant Communications," in *IEEE 58th Conference on Decision and Control*, 2019, pp. 4166–4171.

[14] G. Zhang *et al.*, "Trajectory Optimization and Power Allocation for Multi-Hop UAV Relaying Communications," *IEEE Access*, vol. 6, pp. 48 566–48 576, 2018.

[15] X. Liu *et al.*, "Throughput Optimization of Blocked Data Transmission: A Mobile-Relay-UAV-Assisted Approach," in *IEEE International Conference on Computer and Communications*, 2019, pp. 792–796.

[16] A. Zhou *et al.*, "Robotic Millimeter-Wave Wireless Networks," *IEEE Transactions on Networking*, vol. 28, no. 4, pp. 1534–1549, 2020.

[17] B. Siciliano and O. Khatib, *Springer Handbook of Robotics*, 2nd ed. Springer, 2016, ch. 26, pp. 623–670.

[18] M. W. Mueller *et al.*, "A Computationally Efficient Motion Primitive for Quadrocopter Trajectory Generation," *IEEE Transactions on Robotics*, vol. 31, no. 6, pp. 1294–1310, 2015.

[19] W. L. Stutzman, *Antenna Theory and Design*. John Wiley & Sons, 1981, ISBN: 978-0-470-57664-9.

[20] G. Silano *et al.*, "Power Line Inspection Tasks With Multi-Aerial Robot Systems Via Signal Temporal Logic Specifications," *IEEE Robotics and Automation Letters*, vol. 6, no. 2, pp. 4169–4176, 2021.

[21] G. Silano *et al.*, "Software-in-the-loop simulation for improving flight control system design: a quadrotor case study," in *IEEE International Conference on Systems, Man and Cybernetics*, 2019, pp. 466–471.

[22] G. W. Stewart, *Introduction to Matrix Computations*. Academic Press, 1973, ISBN: 9780126703504.

[23] F. R. Gantmacher, *The theory of matrices*. Chelsea Publishing Company, 1977, ISBN: 9780126703504.